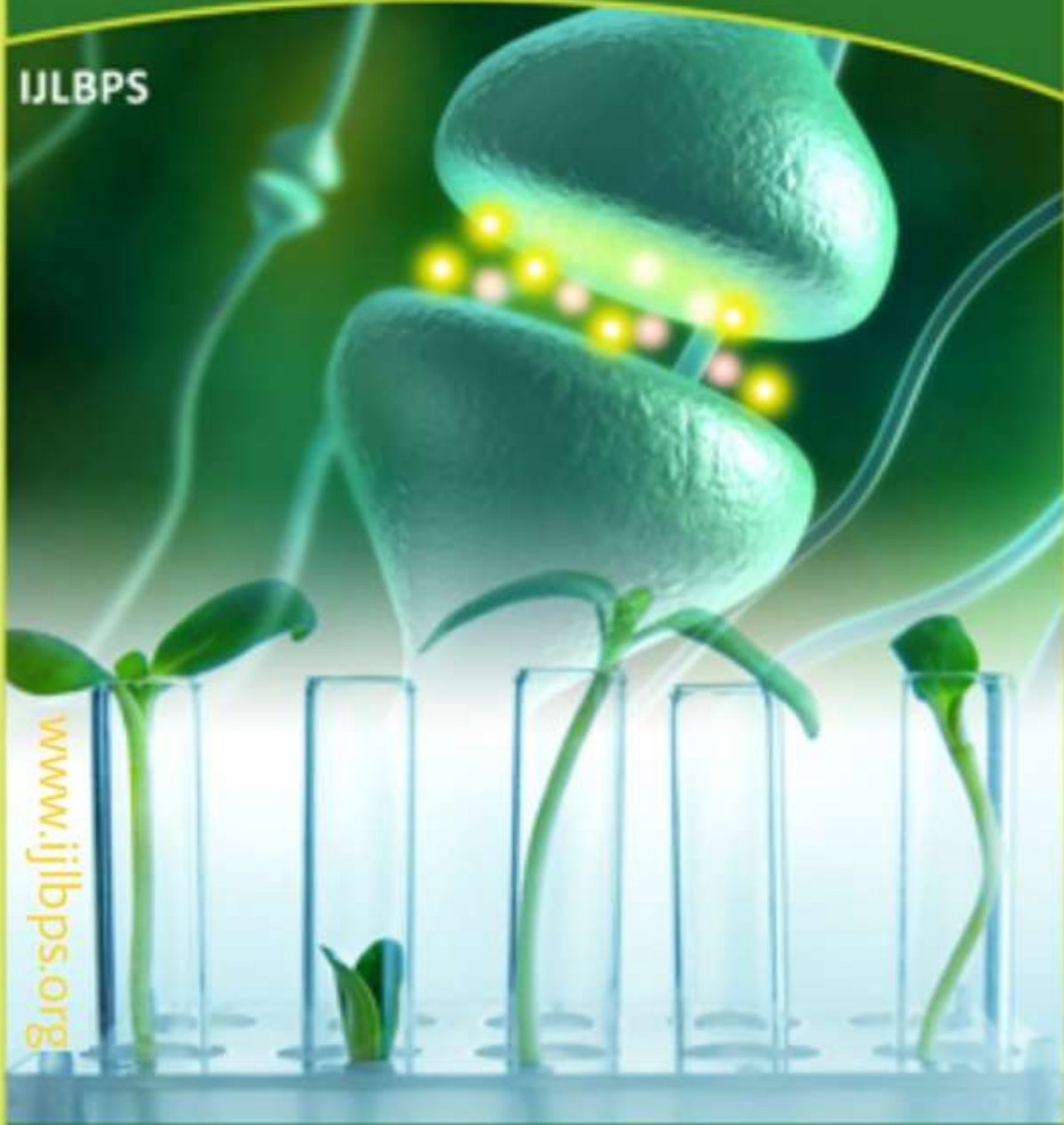




ISSN 2395-650X

International Journal of
Life Sciences Biotechnology Pharma Sciences

IJLBPS



www.ijlbps.org

E-mail: editorijlbps@gmail.com editor@ijlbps.org

A Review of Corrosion and Wear Properties on 316L Stain less Steel

REGUNATH.R

DepartmentOfMechanicalEngineering,SreeVenkateswaraPolytechnicCollege,Kazhudhur,TamilNadu, India

Abstract

A ball-on-disc tribometer was used to test the tribological behavior of 316L stainless steel under various typical loads in dry ambient air using an 85 percent cold rolling process and a subsequent annealing treatment (750 C, 10 min). Friction coefficients were shown to be lower and more stable in 316L stainless steel samples than in coarse-grained samples, especially at higher loads, which may be due to the presence of many oxidative particles at sliding interfaces. corrosion of 316L (UNS S31603) stainless steel expansion joints in the leaching solution of silt on blast furnace gas pipelines in an industrial power plant were studied. TA2's corrosion-resistant qualities indicate that it is the best material for the job. The available literature on various coating kinds and applications has been thoroughly and critically analyzed in this review work.

Keywords: corrosion, tribo-corrosion of 316L stainless steel, adhesion wear, abrasion wear, and oxidativewear;316Lstainlesssteel

1. Introduction

As the Greek word "Tribos" signifies rubbing, tribology is derived from this word, as well. All sections that come into contact with each other are covered. High load, high/low temperature, and harsh chemical environments are among settings where mechanical components have been used in various applications. However, wear is a problem that has been encountered in practically every industry.mechanical/moving components are involved.There are various materials used in modern dentistry that have unique properties in terms of their physical and chemical composition, as well as their aesthetic appeal. In dentistry, 316L stainless steel (AISI classification) is one of the longest-lasting materials on the market today. 316L stainless steel's corrosion resistance and mechanical qualities make it a good choice for shortto medium-term projects.

use in the body for a short period of time Dental 316L is most commonly used in orthodontics to create wires, brackets, and bands for orthodontic braces [2]. As a result of 316L's low price and low toxicity, it is a

popular material for longer-term dental implants in underdeveloped countries.

2. Experimental

2.1. Coating preparation Unbalanced magnetron sputtering deposition in an Ar environment was used to produce the GLC coatings on the WC discs. Beijing Taimi Machinery Co., Ltd. developed the WC substrates with 30 mm x 30 mm x 5 mm dimensions. To achieve a final surface roughness of Ra1410–20 nm, diamond polishing was used on the working surfaces. As a result, the adhesion between Ti and WC substrates was much improved. As previously reported, the deposition was made public.

2.2. Coating characterization A scanning electron microscope was used to examine the microscopic features (SEM, Hitachi S- 4800). To test the mechanical properties, a nano-indenter was used (Nano Indenter II, MTS Ltd., US)

2.3. Tribological performances Areciprocating-typeball-on-disctribo-

meter(CSM,Tribo-S-D0000)wasusedtoinvestigate

In both dry and wet conditions, GLC coatings operate well on brass, aluminum, GCr15, titanium, and other metals. The mechanical properties of the four metallic analogues, all of which had the same diameter of 3 mm, were quite similar. Using the Hertz model for a ball on a flat surface [14,15], the maximum contact pressures were computed. At a load of 5 N, all of the tests were carried out. The greatest sliding speed was 7.86 cm/s and the reciprocating amplitude was 5 mm. Tribo-tests were carried out at least 20,000 times each. The friction coefficients (FCs) were automatically recorded. According to the equation $K14V/SF$ [16], wear rates (WRs) of GLC coatings against different counterparts were determined using the wear volume of GLC coating, S is the entire sliding distance, and F is the normal load. A non-contact 3D (3-dimensional) surface profiler was used to estimate the volume losses of GLC coatings (MicroMAXTM, ADE Phase Shift, AZ US). Wear surfaces were also examined using JSM-5600 SEM, Raman spectroscopy, and electron probe microanalysis (EPMA).

Corrosion Many different solutions, including fake saliva, have been tested in recent investigations to study the micro-abrasion and corrosion mechanisms of type 316L stainless steel. To far, however, there are no research findings to support this.

2.4 Many different solutions, including fake saliva, have been tested in recent investigations to study the micro-abrasion and corrosion mechanisms of type 316L stainless steel. To far, however, there are no research findings to support this.

2.5 Surface Modification with the aid of grafts and implants Surface characteristics of bone implants can be efficiently modified using coating methods. In contrast, these coating methods create a barrier between the substance and its surroundings, preventing the organisms from communicating with each other. Because of this, many of the substrate's beneficial characteristics are rendered ineffective for the species surrounding it. Physically attached to a substrate, these

coatings have a limited binding strength. It is possible to alter the physical and/or chemical properties of the surface by, for example, grafting molecules onto a surface or injecting anions into the substrate's superficial layer. Surface modification methods that do not involve the formation of a coating are described as "non-coating" methods in this section, along with other surface grafting procedures.methods and ion implantation techniques

forthesurfacemodificationofboneimplantmaterials will be introduced. Furthermore, these non-coating techniques do not modify topographic features in either micro- or nano-scale.

2.6 TotalWearThenon-linearrelationshipbetweenappliedloadandmicro-abrasionobserved in this study's results is consistentwith a previous study of 316L stainless steel inartificialsaliva[6].Otherrecentstudiesofdifferent materials and solutions suggest thatapplied electrical potential has no observableeffect on the rate of micro-abrasion [20]. Thisconclusion appears to be consistent with theresultsofthisstudysincethetotalwearofeach appliedloadisconstantforallappliedelectricalpotentials.whichdisplaysthemean totalmicro-abrasionmasschange for eachappliedloadwithastandarderrorshowing thewearvariation over all applied electrical potentials.The'error'showsaverylowvariation between the 5 applied electrical potentials. A standarderror for every electrical potential cannot be generatedbecauseonlyabnormal(unreportable)testresults wererepeated.

2.7 ScanningElectronMicroscopy A XL30 SEM microscope was used to conduct SEM measurements on the coated substrates' surfaces in order to determine the surface morphology.

Secondary and backscattered electron imageswerecollectedat 15 kV

3 MaterialsandMethods

3.1 MaterialsandSpecimens

3.2 For the alloyed material employed, which is to say the substrate material, AISI 316L austenitic stainless steel was used Table

1 shows the chemical makeup of the substance supplied by the manufacturer. An external diameter of 20 mm, an internal diameter of 12 mm, and an overall height of 12 mm were machined into specimens. Finish turning was used to create the outside surface.

3.3 Laser Surface Alloying of 316L Steel

LSA operations were carried out utilizing the re-melting strategy. It went through two stages. As the first phase in the procedure, the alloying substance was applied to the alloyed material (substrate). In order to get a laser-alloyed layer, the alloyed material and its covering were re-melted [32]. Like we said earlier, we used powders to dilute polyvinyl alcohol solution. The generated paste was applied to the exterior cylindrical surfaces of the 316L steel sample. An alloying substance was present in all of the 200-nm-thick layers of coating. The Positector 6000 gauge employed eddy current and magnetic induction to measure the thickness of the coating (DeFelsko, Poznan, Poland). As an alloying agent, the following powders were employed:

Boreal amorphousness

- Mixture of Amorphous Boron and Stellite-6 Powders With Mass Ratio 1:1,
- Mixture of Amorphous Boron and Nickel Powders With Mass Ratio 1:1,
- Mixture of Amorphous Boron and Ni-Cr Powders With Mass Ratio 1:1.

3.4 Microstructure Observations

3.5 The ring-shaped specimens were cut perpendicular to the treated surface, across the laser tracks, following the LSA techniques outlined above. The microstructure of the laser-alloyed samples was studied in the plane perpendicular to the scanning direction by preparing cross sections. In order to create the metallographic specimens, the cut pieces were first put in a conductive resin. Using abrasive paper with varied granularities, they were then polished. During polishing, the Al₂O₃ slurry was finally applied. The laser-alloyed specimens were etched with a specific reagent to disclose their microstructure, which was made from a 25-gram combination

of FeCl₃, 25-mL HCl, and H₂O. (100 mL). Using an optical microscope (OM) Metaval (Carl Zeiss, Poznan, Poland) and a scanning electron microscope (SEM) Vega 5135, the microstructures were studied (TESCAN, Poznan, Poland).

3.6 X-ray Microanalysis and Phase Analysis

Measurements of the concentrations of specified elements in the laser-alloyed layer were made with a 55 utilizing the PGT Avalon X-ray microanalyzer (Princeton Gamma Technology, Poznan, Poland). The content of iron, chromium, nickel, molybdenum, cobalt, and boron were measured. Such elements corresponded to the most important elements of 316L steel (Fe, Cr, Ni, Mo), as well as to the elements, which were the main components of alloying materials (B, Ni, Cr, Co). The accelerating voltage was equal to only 12 kV. It enabled more accurate measurement of such a light element as boron. Si (Li) detector with an ultra-thin window was applied. The standardless quantitative analysis SEM bulk analysis was performed using ZAF (atomic number-absorption-fluorescence) matrix correction techniques. Boron measurements, however, necessitated a unique approach. This procedure's goal was to remove any carbon-based pollution. As a result, genuine standards of boron content were used to calibrate the apparatus. The standards were FeB and Fe₂B phases made on borided Armco iron. There was no carbon dissolution in the iron borides.

3.7 Cohesion

The standard test for determining the adherence of coatings was performed to examine the cohesiveness of laser-alloyed layers. The Rockwell C indentation test was used to determine the surface layer's cohesiveness. Cone-shaped diamonds were used to conduct the experiment.

as in the case of a typical hardness test using this method. The thickness of the sample has to be at least ten times greater than the depth of the indent that was discovered. It's common to see surface fissures and plastic deformation in the substrate after doing the test. An optical microscope (OM) Metaval was used to observe the indents and determine

the level of layer cohesiveness (Carl Zeiss, Poznan, Poland). An eye was trained on any microcracks and probable flaking or delamination that might have occurred as a result of the indentation.

3.8 Anodic and Cathodic Polarization Tests

In a neutral 3.5 percent NaCl solution, anodic and cathodic polarization experiments were performed on 316L stainless steel substrates with and without silane treatments. To ensure a stable potential, the silane-treated samples were maintained in the working solution for at least three hours prior to taking measurements. A platinum mesh and an Ag/AgCl electrode were employed as the counter electrodes. All of the measurements were made at a rate of one millivolt per second between Ag/AgCl and Ag/AgCl.

3.9 Salt Spray Testing

Using a 5 percent sodium chloride solution, the coatings were put through a neutral salt spray test under ASTM B117 to determine their corrosion resistance. Adhesive tape was applied to the specimens' backs and edges prior to exposure. To test the delamination behavior, a fake scratch was produced in the covering and pierced to the alloy substrate. The specimens were taken out of the salt spray chamber on a weekly basis and photographed using a digital camera to capture representative regions. Corrosion performance was evaluated by calculating the time of exposure to the initial incidence of corrosion, measuring corrosion creep from an artificial scratch, and evaluating the coverage with corrosion products from the scratch.

4.3. ELECTROCHEMICAL IMPEDANCE SPECTROSCOPY MEASUREMENTS

Electrochemical impedance spectroscopy measurements (EIS) were employed to monitor the corrosion performance of the silane treated 316L stainless steel substrates in a 3.5 % NaCl solution. EIS measurements were carried out at the open circuit potential, using an Autolab PGSTAT20 instrument. The data were obtained as a function of frequency, using a sine wave of 10mV amplitude peak to peak. A frequency range of 105 Hz to 10⁻² Hz was selected. A three-electrode electrochemical cell arrangement was

used, consisting of the working electrode (4.98cm² of exposed area), Ag/AgCl electrode as reference and platinum as counter electrode.

5. Applications of 316/316L Stainless Steel

- Oil & petroleum refining equipment
- Food processing equipment
- Pulp and paper processing equipment
- Soap and photographic handling equipment

- Textile Industry Equipment
- Architectural
- Pharmaceutical processing equipment

6. Conclusions

A review of the role of 316L stainless steel micro-abrasion-corrosion mechanisms in artificial saliva is presented in this research. The results from the micro-abrasion-corrosion tests were used to generate polarization

- curves, wastage and mechanism maps and to describe the material's tribocorrosion behaviour in a simulated oral environment. It was found that the corrosion resistant nature of 316L stainless steel made its wear

- mechanism micro-abrasion dominated for all test conditions. The superior corrosion resistance of 316L stainless steel has resulted in a micro-abrasion

- rate to be significantly higher than corrosion rate. This was confirmed by the microscopy inspection as any visual signs of surface corrosion had been removed by the micro-abrasion mechanisms

which predominate. The

polarisation curve

results displayed a significant increase in corrosion current

- density in the presence of abrasive particles suggesting the removal of the protective chromium oxide passive film. The micro-abrasion and corrosion weight loss results suggest that the rate of corrosion

- in anodic conditions increases with the increase of micro-abrasion. Repassivation phenomena were

observed in the polarisation curves with higher micro-abrasion. A higher frequency of repassivation was observed for higher rates of micro-abrasion.

References

[1]

Jimmy Mehta, Varinder Kumar Mittal and Pallav Gupta Role of Thermal Spray Coatings on Wear, Erosion and Corrosion Behavior: A Review *Journal of Applied Science and Engineering*, Vol.20, No. 4, pp. 445-452 (2017)

[2] Yan, F.K.; Liu, G.Z.; Tao, N.R.; Lu, K. Strength and ductility of 316L austenitic stainless steel strengthened by nano-scale twin bundles. *Acta Mater.* 2012, 60, 1059–1071.

[3] A. Hayes, S. Sharifi and M.M. Stack Micro-abrasion-corrosion maps of 316L stainless steel in artificial saliva *Corresponding author. E-mail address: Margaret.stack@strath.ac.uk

[4] C. Hodge and M. M. Stack, "Tribocorrosion mechanisms of stainless steel in soft drinks," *Wear*, vol. 270, no. 1, pp. 104–114, 2010.

[5] J. Hutchings, *Tribology, Friction and Wear of Engineering Materials*. Elsevier Limited, 1992, p.284.

[6] M. Stack and M. Mathew, "Micro-abrasion transitions of metallic materials," *Wear*, vol. 255, no. 1–6, pp. 14–22, Aug. 2003.

[7] Yongxin Wang, Liping Wang, Jinlong Lia, Jianmin Chen, Qunji Xue, Tribological properties of graphite-like carbon coatings coupling with different metals in ambient air and water. *Y. Wang et al. / Tribology International* 60(2013)147–155

[8] Field SK, Jarratt M, Teer DG. Tribological properties of graphite-like and diamond-like carbon coatings. *Tribol Int* 2004;37:949–56.

[9] Wenbo Qin¹, Jiajie Kang^{1,*}, Jiansheng Li^{2,*}, Wen Yue¹, Yaoyao Liu³, Dingshun She¹, Qingzhong Mao² and Yusheng Li^{2,*} Tribological Behavior of the 316L Stainless Steel with Heterogeneous Lamella Structure *Materials* 2018, 11, 1839; doi:10.3390/ma11101839

[10] Mohsin Talib Mohammeda*, Zahid A. Khanb, Arshad Noor Siddiqueeb Surface Modifications of Titanium Materials for developing Corrosion Behavior in Human Body Environment: A Review *Mohsin Talib Mohammed et al. / Procedia Materials Science* 6(2014)1610–1618

[11] Michał Kulka^{1,*}, Daria Mikołajczak², Natalia Makuch¹, Piotr Dziarski¹ Laser

Surface Alloying of Austenitic 316L Steel with Boron and Some Metallic Elements: Microstructure *Materials* 2020, 13, 4852; doi:10.3390/ma13214852

[12] B.T. Prayoga, S. Suyitno, R. Dharmastitia

The Wear behavior of UHMWPE against Surface Modified CP-Titanium by Thermal Oxidation

B.T. Prayoga et al., *Tribology in Industry* Vol. 38, No. 4 (2016) 543-551

[13] Nahid Sultan Al-Mamuna, Kashif Mairaj Deenb, Waseem Haidera Corrosion behavior and biocompatibility of additively manufactured 316L stainless steel in a physiological environment: the effect of citrate ions *Additive Manufacturing* 34(2020)101237

[14]

W.S.W. Harun, M.S.I.N. Kamariah, N. Muhammad, S.A.C. Ghani, F. Ahmad, Z. Mohamed, A review of powder additive manufacturing processes for metallic

biomaterials, *Powder Technology*. 327(2018) 128–151, <https://doi.org/10.1016/j.powtec.2017.12.058>.

[15]

P.A. Dearnley, K.L. Dahmand H. Çimenoglu, "The corrosion – wear behaviour of thermally oxidised CP-Ti and Ti–6Al–4V", *Wear*, vol. 256, pp. 469–479, 2004.

[16]

Glaeser, W.A. Steels. In *Materials for Tribology*, 1st ed.; Tribology Series; Elsevier: New York, NY, USA, 1992; Volume 20, pp. 1–260.

[17]

Godec, M.; Donik, C.; Kocijan, A.; Podgornik, B.; Skobir Balantič, D.A. Effect of post-treated low-temperature plasma nitriding on the wear and corrosion resistance of 316L stainless steel manufactured by laser powder bed fusion. *Addit. Manuf.* 2020, 32, 101000.

[18] Arslan E, Totik Y, Demirci E, Alsarar A, 2010. Influence of Surface Roughness on Corrosion and Tribological Behavior of CP-Ti after Thermal Oxidation Treatment. *Journal of Materials Engineering and Performance* 19:428–433.

[19] Yan, F.K.; Liu, G.Z.; Tao, N.R.; Lu, K. Strength and ductility of 316L austenitic stainless steel strengthened by nano-scale twin bundles. *Acta Mater.* 2012, 60, 1059–1071.

[20] Fellah, M.; Labaiz, M.; Assala, O.; Iost, A.; Dekhil, L. Tribological behaviour of AISI 316L stainless steel for biomedical applications. *Tribol. Mater. Surf. Interfaces* 2004, 7, 135–149.

[21] Roohangiz Zandi Zand1, Kim Verbeken2, Annemie Adriaens1,* The corrosion resistance of 316L stainless steel coated with a silane hybrid nanocomposite coating